Immunity
Article

Conduits Mediate Transport of Low-Molecular-Weight Antigen to Lymph Node Follicles

Ramon Roozendaal,[1,3,4] Thorsten R. Mempel,[2,4,5] Lisa A. Pitcher,[1,4] Santiago F. Gonzalez,[1] Admar Verschoor,[1,6] Reina E. Mebius,[3] Ulrich H. von Andrian,[2] and Michael C. Carroll[1,*]

[1]Immune Disease Institute and Departments of Pediatrics and Pathology, Harvard Medical School, 800 Huntington Avenue, Boston, MA 02115, USA

[2]Department of Pathology, Harvard Medical School and Immune Disease Institute, NRB, 77 Avenue Pasteur, Boston, MA 02115, USA

[3]Department of Molecular Cell Biology and Immunology, VU Medical Center, Van der Boechorststraat 7, 1081 BT Amsterdam, The Netherlands

[4]These authors contributed equally to this work

[5]Present address: Center for Immunology and Inflammatory Diseases, Massachusetts General Hospital, 149 13th St, Charlestown, MA 02129, USA

[6]Present address: Institute for Medical Microbiology, Immunology and Hygiene, Technical University Munich, Trogerstrasse 30, 81675 Munich, Germany

*Correspondence: carroll@idi.harvard.edu

DOI 10.1016/j.immuni.2008.12.014

SUMMARY

To track drainage of lymph-borne small and large antigens (Ags) into the peripheral lymph nodes and subsequent encounter by B cells and follicular dendritic cells, we used the approach of multiphoton intravital microscopy. We find a system of conduits that extend into the follicles and mediate delivery of small antigens to cognate B cells and follicular dendritic cells. The follicular conduits provide an efficient and rapid mechanism for delivery of small antigens and chemokines such as CXCL13 to B cells that directly contact the conduits. By contrast, large antigens were bound by subcapsular sinus macrophages and subsequently transferred to follicular B cells as previously reported. In summary, the findings identify a unique pathway for the channeling of small lymph-borne antigens and chemoattractants from the subcapsular sinus directly to the B cell follicles. This pathway could be used for enhancing delivery of vaccines or small molecules for improvement of humoral immunity.

INTRODUCTION

Lymph nodes (LNs) are strategically positioned and functionally partitioned for facilitating the initiation of immune responses to foreign antigens (Ags). Ags drain into the node via the afferent lymph or are delivered by dendritic cells (DCs) (Kissenpfennig et al., 2005). A series of cellular interactions in anatomically distinct compartments of the LN then governs the development of both a cellular and a humoral immune response aimed at the elimination of the eliciting Ag (von Andrian and Mempel, 2003). Whereas T cells rely on processed Ag presented in the context of major histocompatibility complex (MHC) molecules, B cells recognize Ag in its native, unprocessed form via their immunoglobulin (Ig) receptors (Germain, 1994; Rajewsky, 1996). The anatomical site in which B cells first encounter Ag depends on the route of infection, i.e., intravenous (i.v.), mucosal, or subcutaneous (s.c.). Naive B cells circulate through the secondary lymphoid organs, including the spleen and peripheral LNs, to increase the likelihood of Ag encounter (Allen et al., 2007; Hauser et al., 2007; Okada and Cyster, 2006; Schwickert et al., 2007; von Andrian and Mempel, 2003). Their accumulation in the follicular region is controlled by chemokines such as CXCL13, which is secreted by specialized stromal cells, including follicular dendritic cells (FDCs) and follicular stromal cells (FSCs) (Allen and Cyster, 2008; Gunn et al., 1998). On encounter with Ag, B cells are activated and migrate to the T-B cell border, where they interact with cognate T cells (Garside et al., 1998; Okada et al., 2005). Given their central location, FDCs provide an efficient site for retention of Ag that enters via the blood or lymph. Ag is retained chiefly by complement receptors (CD21 and CD35) and Fc receptors (FcγRIIB) (Carroll, 2004; Nimmerjahn and Ravetch, 2006; Tew et al., 1990). Moreover, FDCs foster development of the germinal center reaction once B cells are activated (Cyster et al., 2000; Kosco and Gray, 1992). This specialized environment, in which B cells undergo expansion, class-switch recombination, and somatic hypermutation, promotes differentiation of the Ag-specific B cells into memory or plasma cells (MacLennan, 1994; Kelsoe, 1995; Rajewsky, 1996; Victoratos et al., 2006).

In the spleen, marginal-zone B cells transport Ag into the follicles (Cinamon et al., 2008; Ferguson et al., 2004; Youd et al., 2002; Guinamard et al., 2000; Pozdnyakova et al., 2003). However, LNs lack an equivalent B cell subset. Earlier studies reported transport of Ag into the LN follicles via a subset of subcapsular sinus (SCS) macrophages identified as binding a fusion protein of the N-terminal cysteine-rich (CR) domain of the mannose receptor fused to the Fc region of human IgG ($CRFc^{+}$) (Berney et al., 1999; Martinez-Pomares et al., 1996). In addition, nonphagocytic cells of dendritic appearance have been implicated in Ag transport (Szakal et al., 1983). An alternative mechanism is a system of conduits that permeates both LNs and spleen, yet these are generally considered to mainly supply the T cell areas of the LNs (Gretz et al., 2000; Okada and Cyster,

2006; Sixt et al., 2005). The recent finding that lymph-borne Ags are differentially taken up and subsequently processed according to size suggests a more selective process. Large lymph-borne Ags are bound by SCS macrophages, which line the floor of the LN (Carrasco and Batista, 2007; Junt et al., 2007; Phan et al., 2007) and are made available to the underlying B cell compartment. Thus, cognate B cells survey the SCS for specific Ag while immune complexes (ICs) are taken up by follicular (FO) B cells via complement receptors CD21 and CD35 (Phan et al., 2007). By contrast, small Ags (less than 70 kDa) either enter conduits leading to the paracortical (T cell) area (Sixt et al., 2005) or diffuse via gaps in the SCS floor into the follicles, where they are taken up by cognate B cells (Pape et al., 2007).

To directly compare transport of large and small Ags into the B cell follicles in vivo, we have used a combination of multiphoton intravital microscopy (MP-IVM) (Lindquist et al., 2004; Mempel et al., 2004; Miller et al., 2002; Shakhar et al., 2005), electron microscopy, confocal analyses of cryosections (Carrasco and Batista, 2007; Gretz et al., 2000; Pape et al., 2007; Sixt et al., 2005), and flow-cytometry analyses (FACS) of peripheral LNs (Phan et al., 2007). As reported earlier, large Ags are transported into B cell areas via FO B cells in a complement-dependent manner. By contrast, a novel network of FO conduits was identified that mediates rapid transport of small soluble-protein Ags from the SCS into the B cell follicular region. Moreover, the conduits provide a source of B cell chemokine (CXCL13), which is secreted by FSCs. Together, the results suggest a pathway for channeling small Ags and chemokines into the B cell area.

RESULTS

Differential Transport of Large and Small Ags

To directly compare the uptake of large and small Ags by FDCs, we injected mice s.c. in the hind footpad with a small volume of soluble ICs prepared from fluorescently labeled keyhole limpet hemocyanin (KLH) (large, monomer 450 kDa) or turkey egg lysozyme (TEL) (small, 14 kDa). On cryosections of draining popliteal LNs (pLNs), we identified uptake of TEL on FDCs 6 hr after injection (Figure 1A, right panel). By contrast, negligible amounts of the larger KLH Ag were observed at this time (Figure 1A, left panel). However, by 24 hr after injection, similar amounts of TEL and KLH had accumulated on FDCs (results not shown). Similar results were obtained with mice actively immunized by a previous injection of TEL or passively immunized with specific rabbit polyclonal antisera (results not shown). Because IC formation in situ upon injection of free Ag more closely mimics the physiological process, we passively immunized mice in subsequent experiments by intraperitoneal (i.p) injection of antiserum several hours before s.c. injection of Ag. A similar approach was reported by Phan et al. for tracking uptake and transport of large Ag into the B cell follicles (Phan et al., 2007).

To more closely examine the kinetics of uptake of large and small lymph-borne Ags by FDCs, we injected passively immunized mice s.c. in the hind flanks with an equal molar mixture of large (Phycoerytherin [PE], ~240 kDa) and small (TEL, ~12–14 kDa) Ags. Draining inguinal LNs were harvested at various times for analysis. Both Ags were present in the SCS sinus by 15 min, and small Ag was first observed on FDCs at 2 hr after injection, whereas PE Ag was not observed on FDCs until at least 8 hr, consistent with the report by Phan et al. (Phan et al., 2007) (Figure 1B). By 24 hr, both Ags were observed on FDCs, consistent with our previous finding with KLH and TEL in the pLN. Thus, small Ags are taken up by FDCs more rapidly than large ones in both the pLNs and inguinal LNs, although the process is slower in the latter, probably because of less efficient drainage from the injection site. Small Ag (TEL) injected in nonimmune mice did not detectably bind to FDCs and was not retained in the draining LN (Figure S1 available online).

ICs composed of large Ags such as PE are transported by naive B cells from the SCS into the follicles and transferred to FDCs in a complement-receptor-dependent manner (Phan et al., 2007). To evaluate the relative efficiency of FO B cell transport of large and small Ags, we analyzed by FACS single-cell suspensions prepared from inguinal LNs at varying times after s.c. injection. PE was found on FO B cells as early as 2 hr, peaked at 8 hr, and then decreased at 24 hr after injection (Figure 1C). Uptake was dependent on expression of CD21 and CD35 on FO B cells, given that characterization of Cr2 mixed chimeric mice identified substantially greater amounts of PE Ag on $Cr2^+$ than on $Cr2^-$ B cells, consistent with the report by Phan et al. (Phan et al., 2007) (Figure S2). By contrast, B cell uptake of small Ags was less pronounced, with maximal uptake at 2 hr and subsequent decrease (Figure 1C). Thus, B cell transport of small Ags is not as efficient as with large Ags, yet the former is identified on FDCs within a shorter time period (Figures 1B and 1C). This suggests that small Ags are transported to FDCs by both B cell-dependent and B cell-independent mechanisms.

Conduits Mediate Small-Ag Transport into Follicles

Previous studies on Ag transport in secondary lymphoid organs have identified a system of conduits that originate from the SCS and permeate the interfollicular zone and paracortical T cell area in LNs (Gretz et al., 2000; Sixt et al., 2005). These conduits consist of a core of collagen fibers ensheathed by a basement membrane and a layer of fibroblastic reticular cells (FRCs), forming an inner tubular space accessible to small molecules with a hydrodynamic radius of approximately 4–5 nm or an approximate molecular weight of 70 kDa (Gretz et al., 2000; Sixt et al., 2005; Nolte et al., 2003). Because DCs can sample Ags from conduits, these were first proposed to have an important function in facilitating the presentation of lymph-borne Ags to T cells by conduit-associated DCs (Sixt et al., 2005). In addition, Qi et al. found that DCs could also present intact Ag to B cells when these transit the T zone after entering the LN via high endothelial venules (HEVs) (Qi et al., 2006).

The reticular collagen-fiber network (which, under the illumination conditions required for multiphoton fluorescence excitation, becomes visible because of second-harmonic generation) within B cell follicles is less abundant than that in T cell areas (Gretz et al., 2000). To determine whether collagen fibers in B cell follicles are also associated with conduits and whether these participate in channeling Ag directly into the B cell follicle, we injected nonimmune mice s.c. in the hind footpad with a mixture of TEL (12–14 kDa) conjugated either to the large-molecular-weight (~240 kDa) fluorochrome PE ("large TEL," TEL-PE) or to the small-molecule (~1.2 kDa) dye Alexa Fluor 633 ("small TEL,"

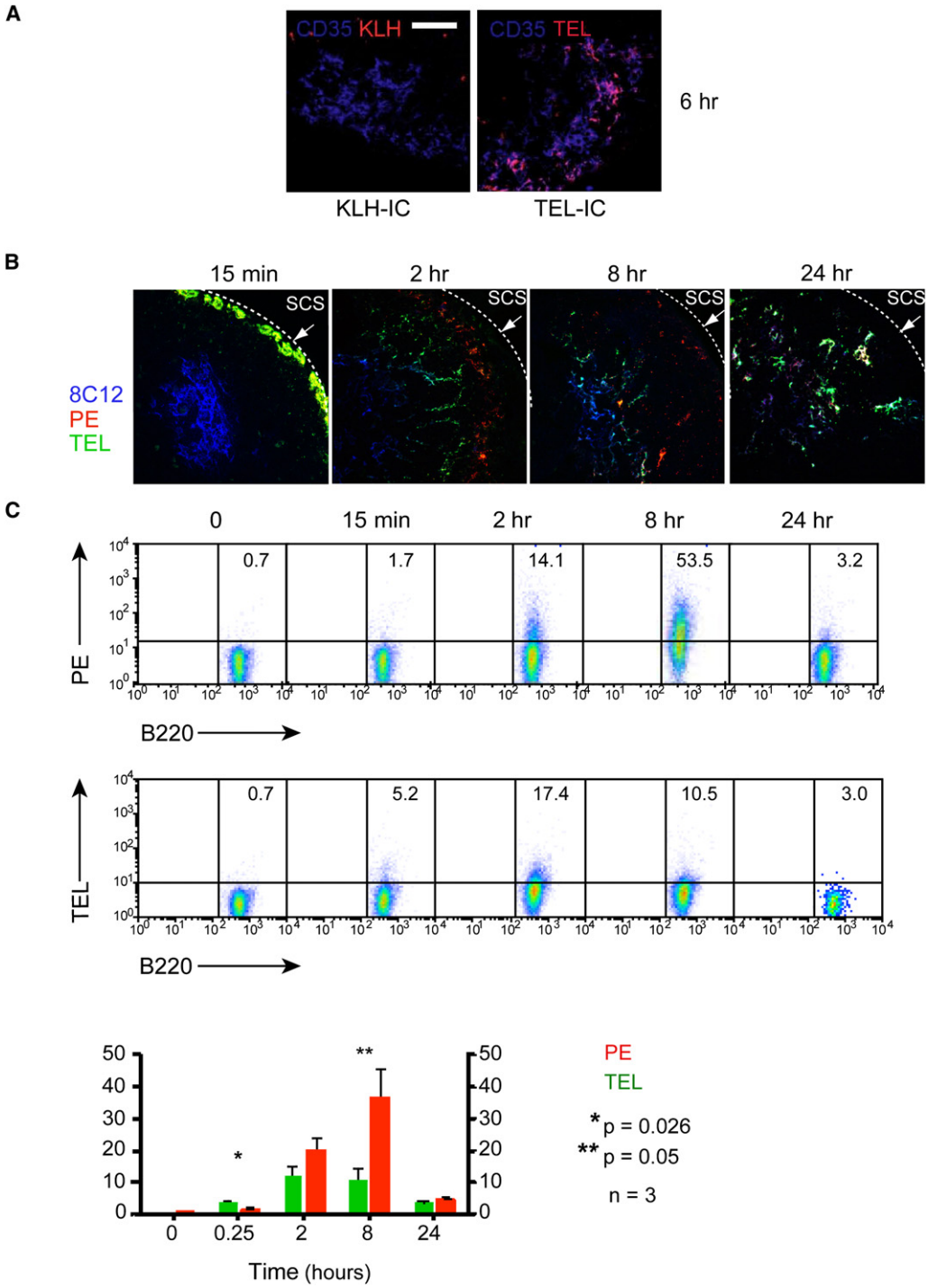

Figure 1. Uptake of Ag on FDCs in Peripheral LNs Is Size Dependent

(A) Confocal fluorescence micrographs of histological sections of pLNs show delay of KLH deposition on FDCs (blue, Cy5-anti-CD35) relative to TEL deposition, 6 hr after injection of IC. The scale bar represents 50 μm. Images are representative of at least three independent experiments.

(B and C) Immunized mice were left untreated (t = 0) or injected with a mixture of 10 μg TEL Alexa 488 and 10 μg B-PE s.c. in the hind flanks.

(B)The draining inguinal LNs were removed at various times, and the deposition of IC on FDCs was analyzed by confocal microscopy with a monoclonal antibody specific for CD35 for labeling FDCs.

(C) In vivo uptake of IC containing small or large Ags by polyclonal B cells was analyzed by FACS. The percentages of $B220^{+}$ cells that have acquired TEL-IC or PE-IC are indicated and are represented in the graph as the mean values ± standard error of the mean (SEM) from at least three LNs. CD45.1+ cells were added during processing of inguinal LNs from CD45.2+ recipient mice for controlling for ex vivo capture of IC. Statistical significance was determined with a one-tailed, paired Student's t test.

A633-TEL) and imaged the pLN by MP-IVM directly thereafter. In addition, to track entry of Ags into the follicles, we seeded recipient mice with fluorescently labeled naive polyclonal primary B cells and with BCR transgenic MD4 B cells that recognize TEL with high affinity. Notably, small TEL was first observed within the SCS and then started to fill FO conduits in a centripetal direction within less than 2 min after injection (Figures 2A and 2B and Movie S1). Importantly, the small Ag became detectable in the interstitial space and on MD4 B cells only with several minutes delay (Figure 2C), suggesting that conduits did not accumulate the Ag from an interstitial pool, but conversely that conduits delivered the Ag to the interstitium. By contrast, the large TEL conjugate was excluded from the conduits, as expected, on the basis of its size (Figures 2A and 2B). The absence of large TEL-PE conjugates from the follicular conduits is consistent with observations of exclusion of proteins of approximate size over 70 kDa (Gretz et al., 2000; Sixt et al., 2005). We noted, though, that at a time point when the concentration of small TEL had reached its maximum in the conduits, large TEL began to slowly penetrate the follicle from the SCS in an interstitial pattern, independent of conduit filling (Figures 2A, 2B, and 2D). We speculate that this delayed entry of the large Ag occurs through a distinct mechanism, possibly by diffusion (Pape et al., 2007) or by binding to non-Ag-specific B cells after shuttling of the Ag across the floor of the SCS (Phan et al., 2007).

To further examine the size exclusion of FO conduits, we injected mice s.c. in the footpad with fluorescently labeled KLH (~450 kDa) and dextrans (of either 40 or 150 kDa molecular weight). Confocal analysis identified localization of these Ags in the SCS within minutes of injection, but only the small, 40 kDa dextran also entered the conduits (Figure S3 and data not shown). Thus, FO conduits appear to have a similar size-exclusion limit as those characterized in the T cell area (Gretz et al., 2000).

Conduits Are Structurally Similar in the T and B Cell Areas

Conduits within the T cell area are characterized by a type I collagen core ensheathed by a fibronectin-containing basement membrane. They are derived from FRCs and are identified by antibodies to ER-TR7 and gp38 (Katakai et al., 2004). To further characterize the conduits in the B cell follicles, we injected naive mice s.c. in the footpad with labeled TEL and immunohistochemically analyzed cryosections of the in situ-fixed draining pLNs. The B cell areas (marked by their central clusters of $CD35^+$ FDCs) contained a network of conduits positive for type I collagen, fibronectin, perlecan, and ER-TR7; this network was, however, less dense than that of T cell areas (Gretz et al., 2000; Sixt et al., 2005) (Figure 3A). Importantly, TEL colocalized with conduits, supporting the MP-IVM results indicating that small Ag drains from the SCS into the follicles via conduits (Figures 3B and 3C). Analysis at higher magnification revealed that TEL is flanked by markers of the conduit-forming FRCs, such as ER-TR7 and gp38, as well as by fibronectin (Figures 3B and 3C). Moreover, TEL was found in association with $CD11c^+$ DCs and $B220^+$ B cells (Figure 3C). These results combined with the observation of size exclusion support the interpretation that small Ags enter the follicles via the FO conduits.

To further characterize the FO conduits, we prepared pLNs from naive mice for ultrastructural analysis. Electron microscopic (EM) examination of the SCS floor and the underlying B cell follicles revealed the presence of conduit structures originating from the floor of the SCS and extending deep into the B cell area (Figure 3D i, ii). The B cell area conduits are composed of bundles of collagen-like fibrils partly wrapped by stromal cells that closely resemble FRCs defined for paracortical conduits (Sixt et al., 2005) (Figure 3D iii, iv). The openings (approximately 1 μm) of conduits to the SCS would provide access for passive drainage of small Ags into the follicles (Figure 3D ii). However, the tightly packed collagen fibers (less than 10 nm spacing) would exclude free diffusion of large molecules. Thus, on the basis of ultrastructural analysis, the conduit structures extending into the B cell area are similar to those identified in the paracortical regions (Gretz et al., 2000; Sixt et al., 2005).

B Cells Rapidly Acquire Small Ag from Conduits

Earlier studies proposed that Ags of a size comparable to that of TEL drain passively via fenestrations in the SCS floor into the underlying follicles, where they are bound by cognate B cells (Pape et al., 2007). Our finding that conduit filling with s.c.-injected TEL precedes the detectable appearance in the interstitium and on B cells (Figure 2C) suggests that conduits might in addition facilitate more efficient direct delivery of Ag to B cells. To test this possibility, we injected limiting amounts of TEL into naive mice that had been seeded with a mixture of fluorescently labeled naive MD4 and polyclonal B cells 20 hr earlier. Under these conditions, only a fraction of MD4 B cells acquired Ag early after injection (Figure 4A and Movie S3), unlike what would be expected if the Ag was distributed through the follicle solely by diffusion. On closer inspection, it was noticed that the majority of Ag^+ B cells were closely associated with an Ag-filled conduit and that the distance from each MD4 B cell to the nearest conduit correlated with the amount of Ag it had acquired (Figures 4A–4C). Moreover, the instantaneous velocity of cognate cells that bound TEL rapidly and transiently declined upon binding of TEL, whereas Ag-free MD4 and control B cells were unaffected (Figure S5 and Movie S1). TEL, like hen lysozyme (HEL), binds MD4 B cells with high affinity. To test whether the rapid kinetics of uptake of the high-affinity Ag TEL is representative of Ag uptake by naive B cells with commonly lower affinity for Ags, we repeated the experiment with duck lysozyme (DEL), which binds the MD4 BCR at 1000-fold lower affinity. Indeed, when a similar amount of DEL was injected s.c. and its entry into the draining pLN was analyzed by MP-IVM, the kinetics of Ag accumulation on MD4 B cells were similar as with the high-affinity TEL Ag (Figure S5 and Movie S4).

One explanation for the increased efficiency of Ag uptake by MD4 cells most proximal to the conduits is that B cells interact directly with conduits, as has been proposed for DCs in the paracortical region (Sixt et al., 2005). Analyses of FO conduits by EM identified gaps in the stromal cell-wrapped conduit, in that the cells appear to "grasp" the conduit without completely enveloping it (Figure 3D i–iii). Inspection of FO conduits by EM identified B cell pseudopods in direct contact with the collagen core (Figure 4D iii). Thus, Ag within the conduits is accessible to FO B cells via the gaps in the FSC envelope.

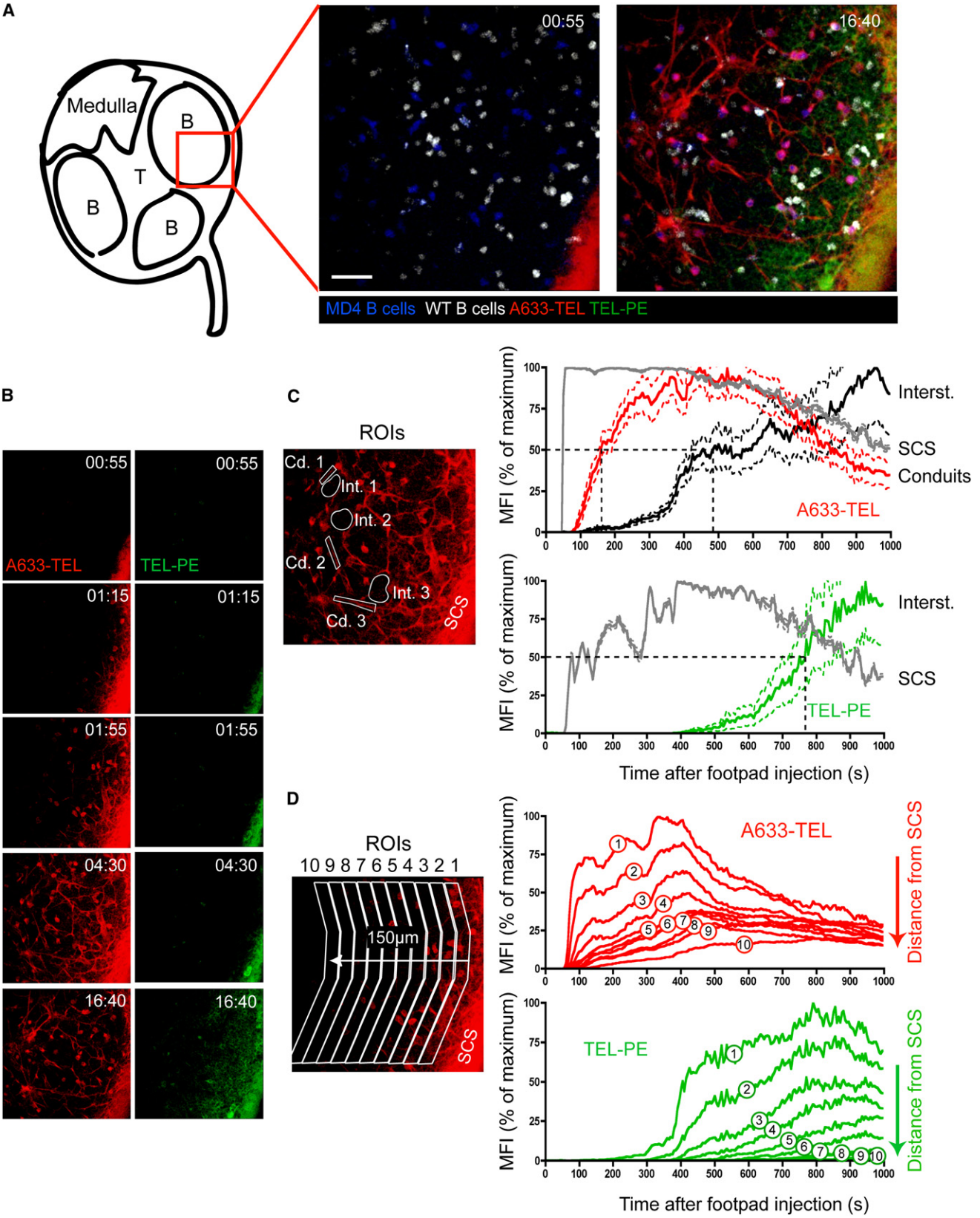
A
Medulla
B
T
B
B
00:55
16:40
MD4 B cells WT B cells A633-TEL TEL-PE
B
00:55
00:55
A633-TEL
TEL-PE
01:15
01:15
01:55
01:55
04:30
04:30
16:40
16:40
C
ROIs
Cd. 1
Int. 1
Int. 2
Cd. 2
Int. 3
Cd. 3
SCS
MFI (% of maximum)
Interst.
SCS
Conduits
A633-TEL
Interst.
SCS
TEL-PE
Time after footpad injection (s)
D
ROIs
10 9 8 7 6 5 4 3 2 1
150µm
SCS
A633-TEL
Distance from SCS
TEL-PE
Distance from SCS
MFI (% of maximum)
Time after footpad injection (s)

Acquisition of Small Ag from Conduits Leads to B Cell Activation

The finding that small Ag enters the follicles via conduits and is rapidly acquired by cognate B cells raised the question of whether Ag trafficking through conduits makes B cell activation more efficient. To compare the relative efficiency of uptake of large TEL-PE and small TEL Ag by cognate B cells, we seeded naive mice with MD4 B cells and then injected them s.c. in the hind flank with a mixture of fluorescently labeled Ag. Inguinal LNs were harvested at various times and analyzed by FACS. Although some MD4 B cells acquired TEL within 30 min after injection, they were devoid of the large Ag TEL-PE. By 60 min, uptake of small TEL by MD4 B cells was maximal, whereas only half as many MD4 B cells acquired TEL-PE. The acquisition of large TEL-PE by the MD4 B cells increased further at both 2 and 4 hr, nearing the maximal levels of small TEL acquired at 60 min. These results indicate that MD4 B cells acquired small TEL more rapidly than the larger Ag when they were coinjected (Figure 4E). Thus, small Ags draining via conduits are more readily accessible to cognate B cells than large Ags entering via other pathways.

To evaluate the quality of the interactions between cognate B cells and their Ag, i.e., whether they led to B cell activation, we seeded wild-type mice with MD4 B cells and 20 hr later injected them separately in the hind flank with either TEL-PE or TEL at equivalent TEL concentrations. Inguinal LNs were harvested at various times, and MD4 B cells were analyzed for upregulation of CD86 as an early marker of activation (Figure 4F). Within 4 hr of Ag encounter, a higher frequency of MD4 B cells upregulated CD86 in response to small TEL as compared to large TEL-PE (Figure 4F). By 6 and 8 hr, approximately equivalent numbers of MD4 B cells that encountered either TEL or TEL-PE had upregulated CD86 (Figure 4F). Thus, B cell activation occurred more rapidly after exposure to small Ag (within 2 hr) compared to MD4 B cells that encountered large TEL-PE.

B cell encounter with cognate Ag leads to their movement to the T-B cell border for interaction with cognate T cells (Garside et al., 1998; Okada et al., 2005), and this approach has been used as an indicator of B cell activation (Carrasco and Batista, 2007; Junt et al., 2007; Pape et al., 2007; Qi et al., 2006). To confirm B cell activation by small, as opposed to large, TEL Ags, we quantified the localization of MD4 cells at the T-B cell border (Figure 4G and Figure S4). In control mice (no Ag), most MD4 B cells were observed within the follicle; only 15% of MD4 B cells were in a follicular border zone (approximately 22 μm inward from the edge of the follicle distal to the SCS) or were extrafollicular. In contrast, in LNs from mice treated with small TEL 8 hr earlier, 51% of MD4 B cells were located in the border and extrafollicular zone, whereas those from TEL-PE-injected mice were similar to cells that had not been exposed to either TEL Ag (Figure 4G and Figure S4). Notably, by 24 hr, a similar percentage of border and extrafollicular MD4 B cells were identified in LNs from TEL or TEL-PE treated mice (Figure S4). These observations indicate that the rapid delivery of TEL via FO conduits results in a more rapid activation of B cells compared to the delayed activation by large Ag, which is excluded from the conduits.

Do FO Conduits Guide B Cells to Ag via CXCL13 Chemokine?

Trafficking of T cells within the paracortical region is not thought to be entirely random but guided by conduit-forming FRCs bearing specific chemokines that promote T cell motility in a haptotactic or haptokinetic fashion (Bajenoff et al., 2006; Mempel et al., 2006; Okada and Cyster, 2007; Worbs et al., 2007). Similarly, CXCL13, produced by stromal cells including FDCs ($CD35^+$) and FSCs ($CD35^-$), probably regulates B cell migration in follicles (Allen and Cyster, 2008; Cyster et al., 2000; Nolte et al., 2003). To examine whether FO conduits harbor CXCL13 in addition to small lymph-borne Ags, we injected naive mice in the footpad with labeled TEL, fixed pLNs in situ, and analyzed cryosections by immunostaining. Staining with anti-CXCL13 identified a reticular pattern within the B cell region that colocalized with both FDCs ($CD35^+$) and conduits (identified by fibronectin and collagen I) (Figures 5A, 5B, and 5C). As expected, the T cell area was negative for CXCL13.

In addition to the conduit-associated reticular pattern, dense CXCL13 staining colocalized with FSCs ($gp38^+$) and FDCs proximal and distal, respectively, to the SCS (Figures 5B and 5C). Moreover, higher-magnification images suggest that the CXCL13 is wrapped by both FDCs and conduit structures (Figure 5C). Thus, the staining pattern suggests that CXCL13 secreted by FSCs enters the conduit and could provide an attractant to guide B cells to a likely site of Ag exposure. However, an alternative interpretation is that FSC-secreted chemokine binds to the outer surface of the FO conduit, as proposed for conduits in the T cell area. Immunostaining of sections from LNs containing labeled TEL identify a similar pattern of staining for fibronectin, CXCL13, and TEL Ag (Figure 5D). Thus, conduits include CXCL13, possibly to provide an attractant to B cells to survey the conduits for the presence of Ag, as proposed for DCs in the T cell area (Bajenoff et al., 2006).

It has been described that chemokines produced at the site of inflammation, such as CCL2, can drain into LNs putatively via

Figure 2. Small Ags Are Rapidly Delivered to LN Follicles through FO Conduits

A633-TEL (red, containing 50 ng TEL) and TEL-PE (green, containing 5 μg TEL) were injected into the footpads of mice, and their entry into the draining LN was monitored by MP-IVM (see also Movie S1).

(A) Intravital micrographs depicting the distribution of the small (A633-TEL, red) and large (TEL-PE, green) Ag in a B follicle early (55 s, left panel) or late (16 min, 40 s, right panel) after footpad injection (WT B = white; MD4 B = blue). The scale bar represents 30 μm.

(B) Micrographs from selected time points depicting either A633-TEL or TEL-PE. Time is shown in minutes and seconds.

(C) Regions of interest (ROIs) were defined for measuring the mean fluorescence intensity (MFI; individually normalized, averaged MFIs ± SEM versus time after TEL injection) of A633-TEL and TEL-PE in the SCS, conduits (Cd. 1–3), and the interstitial space (Int. 1–3). Dotted lines indicate half-maximal values for TEL and TEL-PE in conduits and interstitium.

(D) ROIs with increasing distance from the SCS were defined, and the normalized MFIs of A633-TEL (top panel) and TEL-PE (bottom panel) were plotted against time after injection. This experiment was repeated twice with similar results.

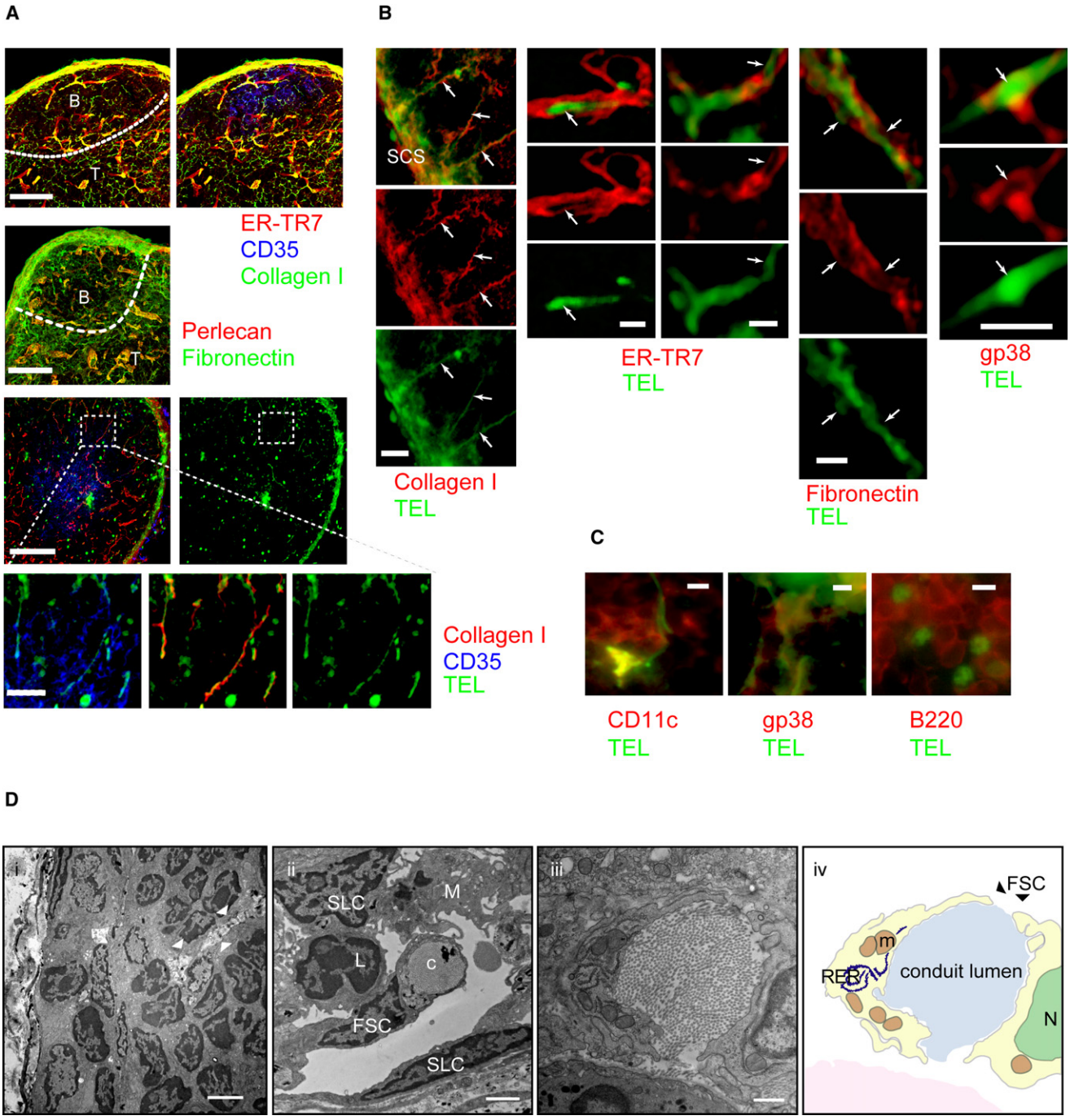

Figure 3. Characterization of the FO Conduits Network by Immunohistology and EM

(A) Imaging of thick cryosections (40 μm) stained for collagen I (green) and ER-TR7 (red) (top panels) or fibronectin (green) and perlecan (red) (middle panels) in B cell follicles. The scale bars represent 100 μm. Hatched lines indicate the T-B cell border. The bottom panels show imaging of thick cryosections after s.c. injection of Ag (TEL, green; collagen I, red; and CD35, blue). The hatched box identifies the area magnified in lower panels. The scale bars represent 100 μm and 20 μm, respectively.

(B) Immunofluoresence on thin cryosections (10 μm) of LN after s.c. injection of Ag (TEL, green). The columns are arranged as follows: left column, collagen I (red [the scale bar represents 20 μm]); second and third columns, ER-TR7 (red); fourth column, fibronectin (red); and fifth column, gp38 (red [scale bars represent 5 μm]).

(C) Ag transported via conduits is acquired by T cell-area dendritic cells (CD11c, left panel, red), FSCs (gp38, middle panel, red), and B cells (B220, right panel, red). Scale bars represent 5 μm.

(D) Ultrastructural characterization of FO conduits. (i) Transmission EM of the SCS and the B cell follicle. The white arrowheads indicate part of a conduit in the B cell follicle. The scale bar represents 1 μm. (ii) Electron micrograph of a conduit (c) in the SCS area. FSC, SLC, and M represent follicular stromal cell, sinus-lining

T cell area conduits in order to influence cellular recruitment via HEVs (Palframan et al., 2001). To further examine a possible role for conduits in the delivery of lymph-borne chemoattractants to the follicles or in the distribution of locally produced chemokines within the B cell area, we injected mice in the footpad s.c. with a small volume of recombinant CCL21 (SLC). LNs were immediately fixed in situ and harvested for analysis. CCL21 is normally found in the T cell area, and, as expected, only a background amount was observed within the B cell follicles in uninjected mice (Figure S7, left panels). By contrast, the follicular zone stained positive for CCL21 within pLNs of mice injected with the chemokine (Figure S7, right panels). Examination of sections at higher magnification revealed CCL21 colocalization with FO conduits (Figure S7). Thus, the results are consistent with a model in which lymph-borne chemoattractants also enter the follicles (and paracortical region) via conduits.

DISCUSSION

It is generally accepted that protein Ags retained on FDCs provide an important depot for encounter by FO B cells (Kosco and Gray, 1992; Kelsoe, 2000; Fu et al., 1997; Cyster et al., 2000; Rajewsky, 1996). How Ag is delivered to FDCs is less clear. Using a combination of MP-IVM, EM, confocal, and flow-cytometric analyses, we observe a unique pathway whereby small soluble Ag drains passively into the B cell zone through a FO conduit system that connects the SCS with FDC areas. Moreover, the FO conduit network, which is less dense but structurally similar to that of the T cell zone, contains CXCL13. Thus, the conduit system provides a source of Ag as well as a possible pathway or network for guiding B cells to Ag within the follicles in a similar manner as identified in the paracortex for T cells.

Qi et al. found that DCs loaded with HEL ex vivo and adoptively transferred into mice present Ag to HEL-specific B cells within the paracortical region (Qi et al., 2006). They proposed that conduit-associated DCs may take up draining Ag and present it to B cells entering the T zone via HEVs. Using a similar model Ag (HEL), Pape et al. tested the importance of DCs in Ag transport in a mouse model in which $CD11c^+$ cells were deleted prior to injection of Ag (Pape et al., 2007). They found that DCs were not essential, given that the HEL drained rapidly into the follicles of the depleted mice and was detected on specific B cells within 3.5 min. They proposed a model in which small protein Ags within the afferent lymph drain directly into the B cell follicles via gaps in the SCS floor and in which cellular transport was not required. Our findings are consistent with their report, given that small Ag drained rapidly into follicles in an apparently cell-independent manner. However, an important difference is that TEL entered the follicles via discrete conduits rather than in a diffuse pattern, representing a second mechanism in which small Ags gain access to the B cell follicles. This discrepancy could result from the different techniques employed to visualize the Ag. In the Pape study, the draining LNs were flash frozen, and cryosections were imaged ex vivo without hydration. In our hands, Ag was only observed inside conduits when LNs were fixed in situ by perfusion via the lymph. It is possible that the flash freezing of the LNs obscured a discrete pattern within FO conduits. Moreover, the conduits, which are readily observed by MP-IVM, are not easily identified by confocal microscopy without staining with specific antibodies.

Immunostaining with antibodies specific for type I collagen identified colocalization of the labeled TEL. Furthermore, staining with Abs specific for basement membrane (fibronectin) or stromal cell surface markers (ER-TR7 and gp38) indicates that the Ag lies within, not outside, the conduit. Interestingly, the conduits appear to merge or overlap with the FDC network, suggesting that small Ags are "delivered" directly and can be taken up if they are tagged with complement ligand C3 (Fang et al., 1998; Fischer et al., 1998). Whether the primary role of conduits is channeling of chemokines and inflammatory mediators or delivery of B cell Ags is not clear. However, our results illustrate that conduits provide an efficient mechanism for delivery of small Ags from the SCS into the follicle, where they are efficiently exposed to B cells.

The finding that TEL is taken up by FDCs more rapidly than larger Ags, such as PE and KLH, which are excluded from conduits, supports our observations that lymph-borne small Ags rapidly fill conduits and drain into the underlying follicles. In contrast, large Ags, such as PE, are bound by FO B cells and delivered to FDCs in a complement-dependent manner, as reported (Phan et al., 2007). However, the uptake of TEL by naive B cells was less efficient, and the peak of uptake occurred earlier than with PE. This suggests that some TEL does diffuse into the follicles and is taken up by B cells as an IC or, alternatively, that TEL Ag enters into the interstitial space after being distributed in the follicle via conduits, as suggested by our MP-IVM results. The observation of TEL entry into follicles via conduits is not explained by an injection of an excessive amount of Ag. In the current study, mice were injected with a mixture of TEL and TEL-PE with less than 1 μg of TEL. This represents considerably less Ag than used by Pape et al. (Pape et al., 2007). Importantly, only the smaller TEL Ag was detected within the FO conduits.

Characterization of the FO conduits by ultrastructural analysis and immunostaining suggests that their structure is similar to that identified for those in the T zone. As reported by Gretz et al. (Gretz et al., 2000), the FO conduits include a core of tightly packed collagen fibrils with spaces of less than 10 nm, which would explain the size exclusion of particles greater than 5.5 nm or approximately 70 kDa. As reported for T zone conduits, conduits in the follicles stained positive for fibronectin and perlecan, suggesting that the collagen core was enveloped by a basement membrane (Sixt et al., 2005). Likewise, the FO conduits stained positive for ER-TR7 and gp38, which are markers for LN stromal cells.

In the current study, FO conduits were found to open into the SCS, which would provide access to small lymph-borne Ags. Although the conduits are "wrapped" by stromal cells, gaps exposing the conduits to B cells were identified. Indeed, MD4 B cells closest to conduits were observed to bind TEL Ag more rapidly than those that were more distal.

cell, and macrophage, respectively. The scale bar represents 2 μm. (iii) Electron micrograph and (iv) schematic drawing of a transverse section of a FSC located in the follicular area of the LN. The high metabolic activity of these cells is indicated by the presence of a prominent rough endoplasmic reticulum (RER) and mitochondria (m); N represents nucleus. The scale bar represents 500 nm.

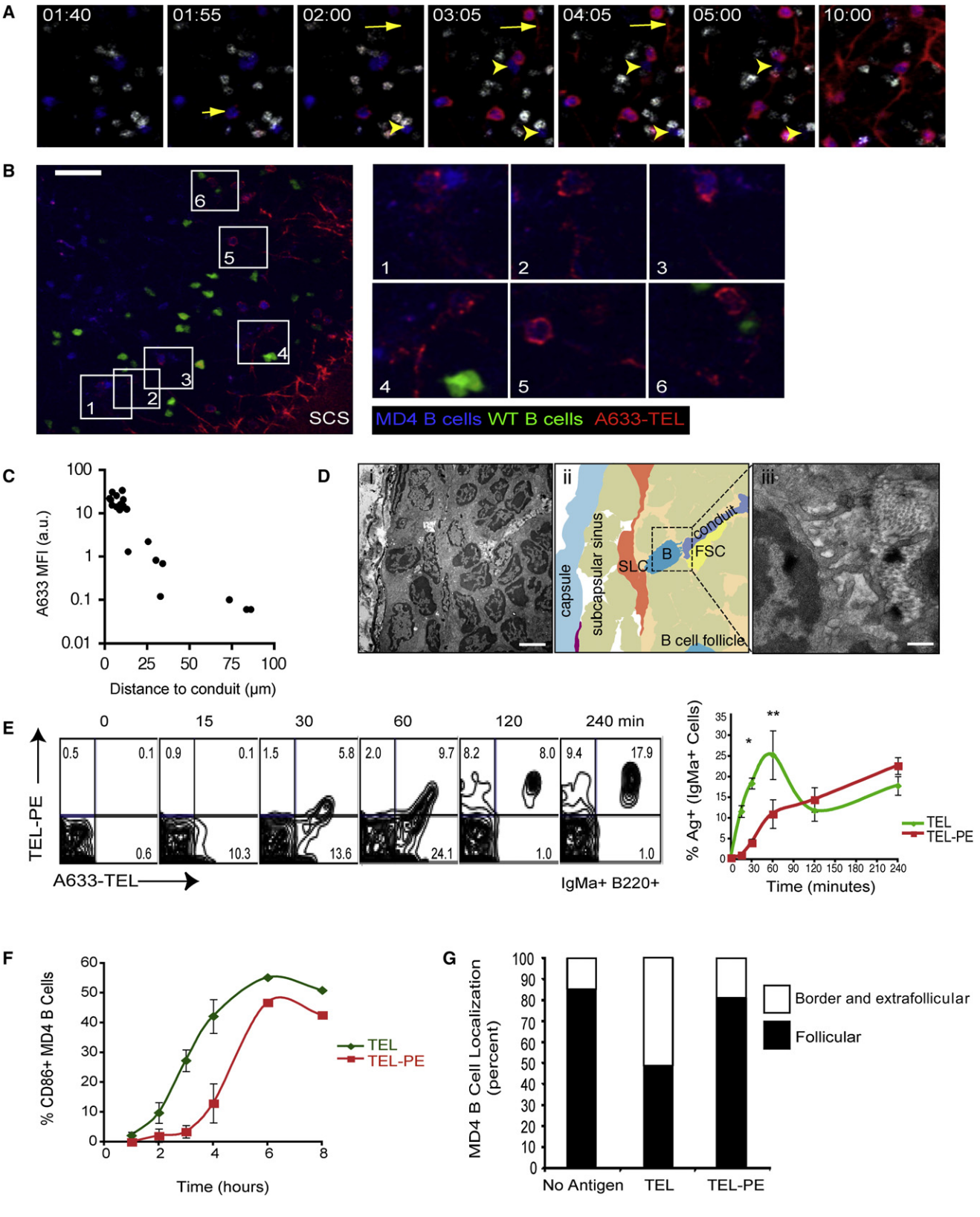
A
01:40
01:55
02:00
03:05
04:05
05:00
10:00
B
SCS
MD4 B cells WT B cells A633-TEL
C
A633 MFI (a.u.)
Distance to conduit (μm)
D
capsule
subcapsular sinus
SLC
B
conduit
FSC
B cell follicle
E
0
15
30
60
120
240 min
TEL-PE
A633-TEL
IgMa+ B220+
% Ag+ (IgMa+ Cells)
Time (minutes)
TEL
TEL-PE
F
% CD86+ MD4 B Cells
Time (hours)
TEL
TEL-PE
G
MD4 B Cell Localization (percent)
Border and extrafollicular
Follicular
No Antigen
TEL
TEL-PE

One difference between conduits in the follicles and those in the T zone is that the former are less dense. One possible explanation for this difference is the presence of the FDC network, which is unique to the follicular region. Thus, the combination of FDC processes and FO conduits would provide a rich network for B cells to interact with Ag.

Rapid transport of small Ag into the follicles via conduits can accelerate its encounter by cognate B cells. Comparison of uptake and activation of MD4 B cells by TEL and TEL-PE revealed more rapid activation by the smaller Ag, on the basis of CD86 expression and earlier migration of activated B cells to the T-B cell border. Moreover, tracking of Ag-bound cognate B cells within the first 15 min after injection of small Ag revealed a dramatic slowing in their migration pattern relative to non-Ag-binding control B cells. In the example of an infectious pathogen, this reduction in response time to microbially derived Ags could provide a substantial benefit to the host (Ochsenbein et al., 1999). Thus, Ag is delivered to the B cell follicles via conduits within minutes after injection and, in the presence of Ig and complement, is taken up on FDCs. These rapid kinetics could be critical in the case of a highly infectious pathogen. Given that intact pathogens exceed the size limit of the conduits, the majority of the microbial Ag could be transported via B cells. However, small secreted bacterial products and/or viral "building blocks" could drain into the B cell zone via the conduits. Moreover, partial degradation of pathogens at the initial site of infection would release smaller products that gain access to the follicles via the FO conduits.

Recently, Bajenoff et al. reported that lymphocytes migrate through the T zone along FRC-ensheathed conduits, presumably in response to chemokines bound to the cell surface (Bajenoff et al., 2006). Likewise, B cells were found to associate with FDC processes, and it was proposed that they are guided by CXCL13. The observation of such a close contact supports a model in which Ag (and complement ligand) is exchanged between the two cell types. In the current study, FO conduits, FSCs, and FDCs colocalized with CXCL13. Staining of cryosections with specific antibody suggests that both FSCs and FDCs are a source of CXCL13, as reported by Cyster et al. (Allen and Cyster, 2008). Thus, one interpretation of our results is that FSCs proximal to the SCS release CXCL13, and from there it permeates the conduit network. Analogous to what has been described in the T cell area (Bajenoff et al., 2006), this would provide a mechanism by which B cells are guided in their migration through B cell follicles by the same structures that deliver Ag draining from peripheral tissues, maximizing their exposure to Ag. Whether CXCL13 enters the conduits or is bound to the outer surface of the FSCs could not be determined definitively from our analysis. However, the finding that CCL21 injected s.c. in the footpad colocalizes with the FO conduits suggests that chemokines like small protein Ags enter follicles via this route.

In summary, we identified a unique network of conduits in peripheral LNs that mediate rapid transport of small soluble-protein Ags from the SCS into the B cell follicular region. The presence of conduits within the follicles provides an efficient mechanism for exposing Ag to B cells and for rapid deposition on FDCs.

EXPERIMENTAL PROCEDURES

Mice

All mice (CD45.1, CD45.2, MD4 [Goodnow et al., 1988], and $Cr2^{-/-}$ [Molina et al., 1996]) were maintained on a C57BL/6 (B6) background and housed at Harvard Medical School and Immune Disease Institute animal facilities under specific pathogen-free conditions. Studies were approved by the institutional animal care and use committees. Mice received food and water ad libitum.

Immunogens and Immunization Protocols

TEL and DEL were purified from fresh turkey eggs (Nicholas Turkey Breeding Farms, Sonoma, CA, USA) as described (Prager and Wilson, 1971). B-PE and KLH were from Sigma Aldrich (St. Louis, MO, USA). Ags were conjugated with Alexa Fluor 488 (A488), 568 (A568), or 633 (A633) carboxylic acid succinimidyl esters (Invitrogen, Carlsbad, CA, USA) according to the manufacturer's instructions. B-PE was covalently coupled to TEL with EDAC (Invitrogen, Carlsbad, CA) and Sulfo-NHS (Pierce Biotechnology, Rockford, IL, USA) and purified by gel filtration chromatography. For in vivo IC formation, mice were passively immunized i.p. with 2 mg rabbit anti-lysozyme (Biodesign, Saco, ME, USA), rabbit anti-KLH (GeneTex, San Antonio, TX, USA), or rabbit anti-B-PE (Rockland, Gilbertsville, PA, USA) and 24 hr later injected s.c. in the hind flanks with a mixture of 10 μg A488-TEL and 10 μg B-PE. The draining inguinal LNs were isolated at various times for flow-cytometry and confocal-microscopy analyses.

Figure 4. Delivery of Ag to B cell by FO Conduits Leads to B cell Activation

(A) A subregion of the same data set as shown in Figure 2 is shown at different time points. The short arrow indicates initial appearance of A633-TEL on a B cell in this region. The long arrow indicates a conduit in which A633-TEL is first detected. The arrowhead indicates MD4 B cells that remain free of or accumulate only minute amounts of A633-TEL. Time is shown in minutes and seconds. See also Movie S2.

(B) A limiting amount of A633-TEL (red, containing 10 ng TEL) was injected into the footpad of a different mouse seeded with MD4 (blue) and WT B cells (green); the draining LN was monitored by MP-IVM (see also Movie S3), and the micrograph was taken 170 s after TEL injection. Magnified regions of interest highlight the close spatial relation of selected TEL^+ MD4 B cells to TEL-containing conduits. The scale bar represents 30 μm.

(C) Quantification of TEL uptake by MD4 B cells (as measured by MFI) as a function of proximity to the nearest TEL^+ conduit. Similar results were obtained in a separate experiment.

(D) Electron micrographs of a B cell follicle (i and iii) and schematic drawing (ii) showing B cell processes in close contact with a conduit. The SLCs that separate the SCS from the B cell follicle are indicated in orange. Scale bars represent 1 μm (i) and 500 nm (iii).

(E) The acquisition of A633-TEL versus TEL-PE by MD4 B cells was assessed over a 4 hr period by FACS. Representative plots, gated on $IgMa^+$ cells that acquired Ag in vivo (labeled MD4 cells were added ex vivo to capture free Ag), from four LNs analyzed in two experiments are shown. Average values ± SEM of Ag acquisition by MD4 B cells are shown in the graph (*p = 0.004, **p = 0.03).

(F) Upregulation of CD86 on MD4 B cells by TEL or TEL-PE. The graph shows percentages of MD4 B cells expressing CD86 at 1, 2, 3, 4, 6, and 8 hr after Ag injection. Average values ± SEM from at least two LNs from three experiments are shown.

(G) Location of MD4 B cells in the inguinal LNs of mice that received no Ag, TEL, or TEL-PE 8 hr earlier. Results from two experiments were analyzed for the numbers of MD4 B cells localized to two zones, one for cells within the follicles and one for cells that were in a ROI within 22 μm of the paracortical-follicular border or extrafollicular, and these data were used for compiling the graph.

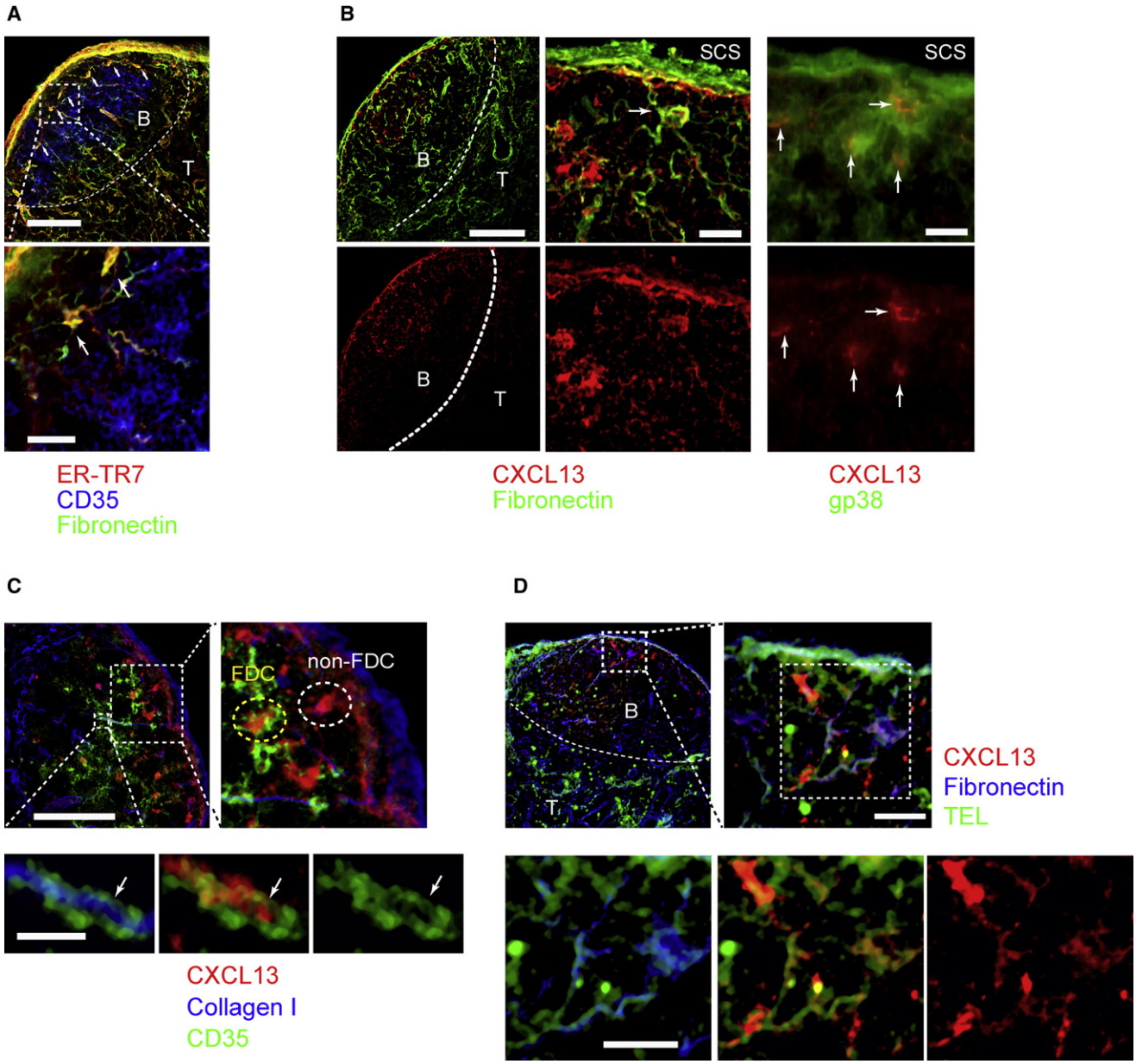

Figure 5. CXCL13 Is Associated with FO Conduits

(A) Immunofluorescence micrographs of B cell follicles stained with antibodies against fibronectin (green), ER-TR7 (red), and CD35 (blue). T-B cell boundaries are indicated by hatched lines. Scale bars represent 100 μm (top) and 20 μm (bottom).

(B) LN cryosections stained for CXCL13 (red), fibronectin (green, left and middle columns [scale bars represent 100 and 20 μm]), and gp38 (green, right column [the scale bar represents 20 μm]).

(C) CXCL13 (red) is localized in lymph node follicles and associates with collagen I (blue) and CD35 (green). Hatched boxes indicate magnified areas. Scale bars represent 100 μm for overview and 20 μm and 5 μm for large and small magnified areas, respectively.

(D) Antigen (TEL, green) and CXCL13 (red) colocalize in a conduit-like pattern with fibronectin (blue). Hatched boxes indicate magnified areas. Scale bars represent 100 μm for overview and 20 μm for magnified areas.

Antibodies

The following antibodies were used for flow cytometry and immunohistochemistry: αCD3ε-Biotin, αCD19-PE, αCD21/35-FITC (7G6), αCD35-Cy5 (8C12), αCD35-Biotin, αCD45.1-PE and FITC, αCD45.2-FITC, αB220-PerCP, αIgM^a-Biotin and Streptavidin-APC (BD Biosciences, San Jose, CA, USA); αB220-Pacific Blue, αCD86-Biotin, Streptavidin-PE/Cy7 (eBiosciences, San Diego, CA, USA); αB220-Cy5, goat anti-rabbit IgG-A488 (Invitrogen); αcollagen I (Chemicon, Temecula, CA, USA); αperlecan and αfibronectin (Neomarkers, Fremont, CA, USA); and αCXCL13-Biotin (R&D Systems, Minneapolis, MN, USA). Antibodies specific for ER-TR7, CD35 (8C12), gp38 (8.1.1), CD11c (N418), and B220 (6B2) were produced in house and conjugated to A488 or A647 or detected with the appropriate Alexa-labeled secondary staining reagents.

Single-Cell Suspensions and FACS Analysis

Single-cell suspensions from LNs were blocked with anti-FcR (2.4G2) and stained with antibodies listed above in PBS containing 1% fetal bovine serum.

Either FACSCalibur or a FACSAria (BD Biosciences, San Jose, CA, USA) flow cytometer and FlowJo software (Tree Star, Ashland, OR, USA) were used for analysis.

Histology

Cryosections of OCT (Tissue tek, Torrence, CA, USA)-embedded LN were prepared as described (Verschoor et al., 2001) and incubated with anti-FcR (2.4G2) before treatment with antibodies listed above in Earle's balanced salt solution containing 1.5% bovine serum albumin and 0.1% saponin for conduit components and CXCL13. Images were acquired with a DM6000 fluorescence microscope and an SP2 confocal microscope (Leica Microsystems, Wetzlar, Germany) and processed with Leica image viewer, Adobe Photoshop, and ImageJ software. In some cases, pseudocolor channels were swapped for visual representation.

B Cell Isolations, Labeling, and Adoptive Transfers

Naive ($CD43^-$) B cells from WT and MD4 spleens were magnetically enriched (Miltenyi Biotec, Auburn, CA, USA) to more than 90% purity. For MP-IVM studies, splenocytes were labeled with CellTracker dyes (Invitrogen), CMFDA at 2.5 μM or CMAC at 20 μM, for 15 min, followed by extensive washing prior to B cell isolation. Recipient mice received a 1:1 mixture of labeled WT and MD4 B cells (3×10^7 cells/mouse) or MD4 only (1.5×10^7) for Ag uptake and B cell activation assays i.v. at least 20 hr prior to Ag injection.

Multiphoton Intravital Microscopy

MP-IVM was performed as described (Mempel et al., 2004). For detailed methods, see Supplemental Experimental Procedures.

Electron-Microscopic Analysis

pLNs were dissected and fixed in 2% formaldehyde or 2.5% glutaraldehyde in 0.1 M sodium cacodylate buffer (pH 7.4) overnight at 4°C. LNs were washed in cacodylate buffer and osmicated with 1% osmium tetroxide and 1.5% potassium ferrocyanide (in water) for 1 hr at 18°C–22°C in the dark. LNs were washed in water and then in 0.05 M maleate buffer (pH 5.15), counterstained for 2 hr in 1% uranyl acetate in maleate buffer, and washed in water. The samples were dehydrated by incubation for 15 min in ethanol in water (60%, 90%, and 100%), incubated in propylene oxide for 1 hr, and transferred into Epon mixed 1:1 with propylene oxide at room temperature overnight. The samples were moved to an embedding mold filled with freshly mixed Epon and heated for 24–48 hr at 0°C for polymerization. Samples were analyzed on a Tecnai G2 Spirit BioTWIN electron microscope (FEI Company, Hillboro, Oregon, USA) at the Harvard Medical School EM Facility.

SUPPLEMENTAL DATA

Supplemental Data include Supplemental Experimental Procedures, seven figures, and four movies and can be found with this article online at http://www.immunity.com/supplemental/S1074-7613(09)00063-6.

ACKNOWLEDGMENTS

We wish to thank D. Vargas for exceptional animal care, R. Yeamans for technical assistance, and N. Barteneva at the IDI Flow and Imaging Cytometry Core facility and M. Ericsson at the Harvard Medical School EM Facility for technical assistance. R.R. is supported by a Marie Curie Fellowship (008873). M.C.C. is supported by a grant from the National Institutes of Health (AI 039246).

Received: August 11, 2008
Revised: November 13, 2008
Accepted: December 10, 2008
Published online: January 29, 2009

REFERENCES

Allen, C.D., and Cyster, J.G. (2008). Follicular dendritic cell networks of primary follicles and germinal centers: Phenotype and function. Semin. Immunol. *20*, 14–25.

Allen, C.D., Okada, T., Tang, H.L., and Cyster, J.G. (2007). Imaging of germinal center selection events during affinity maturation. Science *315*, 528–531.

Bajenoff, M., Egen, J.G., Koo, L.Y., Laugier, J.P., Brau, F., Glaichenhaus, N., and Germain, R.N. (2006). Stromal cell networks regulate lymphocyte entry, migration, and territoriality in lymph nodes. Immunity *25*, 989–1001.

Berney, C., Herren, S., Power, C.A., Gordon, S., Martinez-Pomares, L., and Kosco-Vilbois, M.H. (1999). A member of the dendritic cell family that enters B cell follicles and stimulates primary antibody responses identified by a mannose receptor fusion protein. J. Exp. Med. *190*, 851–860.

Carrasco, Y.R., and Batista, F.D. (2007). B cells acquire particulate antigen in a macrophage-rich area at the boundary between the follicle and the subcapsular sinus of the lymph node. Immunity *27*, 160–171.

Carroll, M.C. (2004). The complement system in regulation of adaptive immunity. Nat. Immunol. *5*, 981–986.

Cinamon, G., Zachariah, M.A., Lam, O.M., Foss, F.W., Jr., and Cyster, J.G. (2008). Follicular shuttling of marginal zone B cells facilitates antigen transport. Nat. Immunol. *9*, 54–62.

Cyster, J.G., Ansel, K.M., Reif, K., Ekland, E.H., Hyman, P.L., Tang, H.L., Luther, S.A., and Ngo, V.N. (2000). Follicular stromal cells and lymphocyte homing to follicles. Immunol. Rev. *176*, 181–193.

Fang, Y., Xu, C., Fu, Y., Holers, V.M., and Molina, H. (1998). Expression of complement receptors 1 and 2 on follicular dendritic cells is necessary for the generation of a strong antigen-specific IgG response. J. Immunol. *160*, 5273–5279.

Ferguson, A.R., Youd, M.E., and Corley, R.B. (2004). Marginal zone B cells transport and deposit IgM-containing immune complexes onto follicular dendritic cells. Int. Immunol. *16*, 1411–1422.

Fischer, M.B., Goerg, S., Shen, L., Prodeus, A.P., Goodnow, C.C., Kelsoe, G., and Carroll, M.C. (1998). Dependence of germinal center B cells on expression of CD21/CD35 for survival. Science *280*, 582–585.

Fu, Y.X., Molina, H., Matsumoto, M., Huang, G., Min, J., and Chaplin, D.D. (1997). Lymphotoxin-alpha (LTalpha) supports development of splenic follicular structure that is required for IgG responses. J. Exp. Med. *185*, 2111–2120.

Garside, P., Ingulli, E., Merica, R.R., Johnson, J.G., Noelle, R.J., and Jenkins, M.K. (1998). Visualization of specific B and T lymphocyte interactions in the lymph node. Science *281*, 96–99.

Germain, R.N. (1994). MHC-dependent antigen processing and peptide presentation: Providing ligands for T lymphocyte activation. Cell *76*, 287–299.

Goodnow, C.C., Crosbie, J., Adelstein, S., Lavoie, T.B., Smith-Gill, S.J., Brink, R.A., Pritchard-Briscoe, H., Wotherspoon, J.S., Loblay, R.H., Raphael, K., et al. (1988). Altered immunoglobulin expression and functional silencing of self-reactive B lymphocytes in transgenic mice. Nature *334*, 676–682.

Gretz, J.E., Norbury, C.C., Anderson, A.O., Proudfoot, A.E., and Shaw, S. (2000). Lymph-borne chemokines and other low molecular weight molecules reach high endothelial venules via specialized conduits while a functional barrier limits access to the lymphocyte microenvironments in lymph node cortex. J. Exp. Med. *192*, 1425–1440.

Guinamard, R., Okigaki, M., Schlessinger, J., and Ravetch, J.V. (2000). Absence of marginal zone B cells in Pyk-2-deficient mice defines their role in the humoral response. Nat. Immunol. *1*, 31–36.

Gunn, M.D., Ngo, V.N., Ansel, K.M., Ekland, E.H., Cyster, J.G., and Williams, L.T. (1998). A B-cell-homing chemokine made in lymphoid follicles activates Burkitt's lymphoma receptor-1. Nature *391*, 799–803.

Hauser, A.E., Shlomchik, M.J., and Haberman, A.M. (2007). In vivo imaging studies shed light on germinal-centre development. Nat. Rev. Immunol. *7*, 499–504.

Junt, T., Moseman, E.A., Iannacone, M., Massberg, S., Lang, P.A., Boes, M., Fink, K., Henrickson, S.E., Shayakhmetov, D.M., Di Paolo, N.C., et al. (2007). Subcapsular sinus macrophages in lymph nodes clear lymph-borne viruses and present them to antiviral B cells. Nature *450*, 110–114.

Katakai, T., Hara, T., Sugai, M., Gonda, H., and Shimizu, A. (2004). Lymph node fibroblastic reticular cells construct the stromal reticulum via contact with lymphocytes. J. Exp. Med. *200*, 783–795.

Kelsoe, G. (1995). The germinal center reaction. Immunol. Today *16*, 324–325.

Kelsoe, G. (2000). Studies of the humoral immune response. Immunol. Res. *22*, 199–210.

Kissenpfennig, A., Henri, S., Dubois, B., Laplace-Builhe, C., Perrin, P., Romani, N., Tripp, C.H., Douillard, P., Leserman, L., Kaiserlian, D., et al. (2005). Dynamics and function of Langerhans cells in vivo: Dermal dendritic cells colonize lymph node areas distinct from slower migrating Langerhans cells. Immunity *22*, 643–654.

Kosco, M.H., and Gray, D. (1992). Signals involved in germinal center reactions. Immunol. Rev. *126*, 63–76.

Lindquist, R.L., Shakhar, G., Dudziak, D., Wardemann, H., Eisenreich, T., Dustin, M.L., and Nussenzweig, M.C. (2004). Visualizing dendritic cell networks in vivo. Nat. Immunol. *5*, 1243–1250.

MacLennan, I.C. (1994). Germinal centers. Annu. Rev. Immunol. *12*, 117–139.

Martinez-Pomares, L., Kosco-Vilbois, M., Darley, E., Tree, P., Herren, S., Bonnefoy, J.Y., and Gordon, S. (1996). Fc chimeric protein containing the cysteine-rich domain of the murine mannose receptor binds to macrophages from splenic marginal zone and lymph node subcapsular sinus and to germinal centers. J. Exp. Med. *184*, 1927–1937.

Mempel, T.R., Henrickson, S.E., and Von Andrian, U.H. (2004). T-cell priming by dendritic cells in lymph nodes occurs in three distinct phases. Nature *427*, 154–159.

Mempel, T.R., Junt, T., and von Andrian, U.H. (2006). Rulers over randomness: Stroma cells guide lymphocyte migration in lymph nodes. Immunity *25*, 867–869.

Miller, M.J., Wei, S.H., Parker, I., and Cahalan, M.D. (2002). Two-photon imaging of lymphocyte motility and antigen response in intact lymph node. Science *296*, 1869–1873.

Molina, H., Holers, V.M., Li, B., Fung, Y., Mariathasan, S., Goellner, J., Strauss-Schoenberger, J., Karr, R.W., and Chaplin, D.D. (1996). Markedly impaired humoral immune response in mice deficient in complement receptors 1 and 2. Proc. Natl. Acad. Sci. USA *93*, 3357–3361.

Nimmerjahn, F., and Ravetch, J.V. (2006). Fcgamma receptors: Old friends and new family members. Immunity *24*, 19–28.

Nolte, M.A., Belien, J.A., Schadee-Eestermans, I., Jansen, W., Unger, W.W., van Rooijen, N., Kraal, G., and Mebius, R.E. (2003). A conduit system distributes chemokines and small blood-borne molecules through the splenic white pulp. J. Exp. Med. *198*, 505–512.

Ochsenbein, A.F., Pinschewer, D.D., Odermatt, B., Carroll, M.C., Hengartner, H., and Zinkernagel, R.M. (1999). Protective T cell-independent antiviral antibody responses are dependent on complement. J. Exp. Med. *190*, 1165–1174.

Okada, T., and Cyster, J.G. (2006). B cell migration and interactions in the early phase of antibody responses. Curr. Opin. Immunol. *18*, 278–285.

Okada, T., and Cyster, J.G. (2007). CC chemokine receptor 7 contributes to Gi-dependent T cell motility in the lymph node. J. Immunol. *178*, 2973–2978.

Okada, T., Miller, M.J., Parker, I., Krummel, M.F., Neighbors, M., Hartley, S.B., O'Garra, A., Cahalan, M.D., and Cyster, J.G. (2005). Antigen-engaged B cells undergo chemotaxis toward the T zone and form motile conjugates with helper T cells. PLoS Biol. *3*, e150.

Palframan, R.T., Jung, S., Cheng, G., Weninger, W., Luo, Y., Dorf, M., Littman, D.R., Rollins, B.J., Zweerink, H., Rot, A., and von Andrian, U.H. (2001). Inflammatory chemokine transport and presentation in HEV: A remote control mechanism for monocyte recruitment to lymph nodes in inflamed tissues. J. Exp. Med. *194*, 1361–1373.

Pape, K.A., Catron, D.M., Itano, A.A., and Jenkins, M.K. (2007). The humoral immune response is initiated in lymph nodes by B cells that acquire soluble antigen directly in the follicles. Immunity *26*, 491–502.

Phan, T.G., Grigorova, I., Okada, T., and Cyster, J.G. (2007). Subcapsular encounter and complement-dependent transport of immune complexes by lymph node B cells. Nat. Immunol. *8*, 992–1000.

Pozdnyakova, O., Guttormsen, H.K., Lalani, F.N., Carroll, M.C., and Kasper, D.L. (2003). Impaired antibody response to group B streptococcal type III capsular polysaccharide in C3- and complement receptor 2-deficient mice. J. Immunol. *170*, 84–90.

Prager, E.M., and Wilson, A.C. (1971). The dependence of immunological cross-reactivity upon sequence resemblance among lysozymes. I. Microcomplement fixation studies. J. Biol. Chem. *246*, 5978–5989.

Qi, H., Egen, J.G., Huang, A.Y., and Germain, R.N. (2006). Extrafollicular activation of lymph node B cells by antigen-bearing dendritic cells. Science *312*, 1672–1676.

Rajewsky, K. (1996). Clonal selection and learning in the antibody system. Nature *381*, 751–758.

Schwickert, T.A., Lindquist, R.L., Shakhar, G., Livshits, G., Skokos, D., Kosco-Vilbois, M.H., Dustin, M.L., and Nussenzweig, M.C. (2007). In vivo imaging of germinal centres reveals a dynamic open structure. Nature *446*, 83–87.

Shakhar, G., Lindquist, R.L., Skokos, D., Dudziak, D., Huang, J.H., Nussenzweig, M.C., and Dustin, M.L. (2005). Stable T cell-dendritic cell interactions precede the development of both tolerance and immunity in vivo. Nat. Immunol. *6*, 707–714.

Sixt, M., Kanazawa, N., Selg, M., Samson, T., Roos, G., Reinhardt, D.P., Pabst, R., Lutz, M.B., and Sorokin, L. (2005). The conduit system transports soluble antigens from the afferent lymph to resident dendritic cells in the T cell area of the lymph node. Immunity *22*, 19–29.

Szakal, A.K., Holmes, K.L., and Tew, J.G. (1983). Transport of immune complexes from the subcapsular sinus to lymph node follicles on the surface of nonphagocytic cells, including cells with dendritic morphology. J. Immunol. *131*, 1714–1727.

Tew, J.G., Kosco, M.H., Burton, G.F., and Szakal, A.K. (1990). Follicular dendritic cells as accessory cells. Immunol. Rev. *117*, 185–211.

Verschoor, A., Brockman, M.A., Knipe, D.M., and Carroll, M.C. (2001). Cutting edge: Myeloid complement C3 enhances the humoral response to peripheral viral infection. J. Immunol. *167*, 2446–2451.

Victoratos, P., Lagnel, J., Tzima, S., Alimzhanov, M.B., Rajewsky, K., Pasparakis, M., and Kollias, G. (2006). FDC-specific functions of p55TNFR and IKK2 in the development of FDC networks and of antibody responses. Immunity *24*, 65–77.

von Andrian, U.H., and Mempel, T.R. (2003). Homing and cellular traffic in lymph nodes. Nat. Rev. Immunol. *3*, 867–878.

Worbs, T., Mempel, T.R., Bolter, J., von Andrian, U.H., and Forster, R. (2007). CCR7 ligands stimulate the intranodal motility of T lymphocytes in vivo. J. Exp. Med. *204*, 489–495.

Youd, M.E., Ferguson, A.R., and Corley, R.B. (2002). Synergistic roles of IgM and complement in antigen trapping and follicular localization. Eur. J. Immunol. *32*, 2328–2337.